OVID: OPEN-VOCABULARY INTRUSION DETECTION

Anonymous authors
Paper under double-blind review

ABSTRACT

Various vision intrusion detection models have made great success in many scenarios, *e.g.*, autonomous driving, intelligent monitoring and security. However, their reliance on pre-defined classes limits their applicability in open-world intrusion detection scenarios. To remedy these, we introduce the *O*pen-*V*ocabulary *I*ntrusion *D*etection (OVID) project for the first time. Specifically, we first develop a novel dataset named Cityintrusion-OpenV for OVID, with more diverse intrusion categories and corresponding text prompts. Then, we design a multi-modal, multi-task, and end-to-end open-vocabulary intrusion detection framework named OVIDNet. It achieves open-world intrusion detection via aligning visual features with language embeddings. Further, two simple yet effective strategies are proposed to improve the generalization and performance of this specific task: (1) A **M**ulti-**D**istributed **N**oise **M**ixing strategy is introduced to enhance location information of unknown and unseen categories. (2) A **D**ynamic **M**emory-**G**ated module is designed to capture the contextual information under complex scenarios. Finally, comprehensive experiments and comparisons are conducted on multiple dominant datasets, *e.g.*, COCO, Cityscape, Foggy-Cityscape, and Cityintrusion-OpenV. Besides, we also evaluate the universal applicability of our model in real scenarios. The results show that our method can outperform other classic and promising methods, and reach strong performance even under task-specific transfer and zero-shot settings, demonstrating its high practicality. All the source codes and datasets will be released.

1 INTRODUCTION

Vision-based intrusion detection tasks have numerous applications in life, *i.e.*, security, intelligent monitoring, and autonomous driving (Ye et al., 2024; Sun et al., 2020). Intrusion detection aims to determine whether potential objects go into a specific restricted Area-of-Interest (AoI) (Sun et al., 2020; Shi et al., 2022). Based on whether the camera is moving or not, intrusion detection tasks can be divided into static and dynamic intrusion detection. Static intrusion detection is relatively easy due to the fixed AoI and achieves great progress by some promising strategies, *e.g.*, Histogram of Oriented Gradients (HOG) (Zhang et al., 2015), Conditional Random Field (CRF) (Matern et al., 2013), Adaptive Background Subtraction (ABS) (Stauffer & Grimson, 2000). However, static intrusion detection can not meet the requirements of *real-time* and *accuracy* under dynamic scenes. Fortunately, with the continuous development of computer vision, some promising detection and segmentation frameworks are proposed (Wang et al., 2023; Chen et al., 2018), which provide new schemes and paradigms for solving the problem of dynamic-view intrusion detection, *i.e.*, based on *overlapping pixel points* between objects and AoI (Sun et al., 2020; Shi et al., 2022). Nevertheless, these proposed models can only detect a single intrusion category, *i.e.*, **Pedestrians**. Considering the lack of sufficient practicality, MF-ID (Han et al., 2024b) and MMID-bench (Han et al., 2024c) propose the first concept and task of multi-category and multi-domains intrusion detection, which successfully extends the intrusion categories and domains, *i.e.*, **1**→**4**. Meanwhile, Ada-iD (Han et al., 2024a) proposes a new active domain adaptation intrusion detection method to further improve the performance of intrusion detection in adverse environments. Although these promising works extend the intrusion categories and scenarios by effective strategies, *e.g.*, Unsupervised Domain Adaptation, Active Domain Adaptation, their reliance on pre-defined object classes limits their applicability in **Open-World** intrusion detection scenarios, as shown in Figure 1. A pre-defined intrusion detection framework can only detect specific or labeled categories in training sets and can not detect categories unseen and undefined, which severely limits the practicality of intrusion detection.

For some unseen intrusion categories, *e.g.*, Car or Truck, the previous models can not give correct intrusion detection results. To address this problem, we propose the **O**pen **V**ocabulary **I**ntrusion **D**etection, namely **OVID**, to detect unseen and undefined intrusion categories effectively.

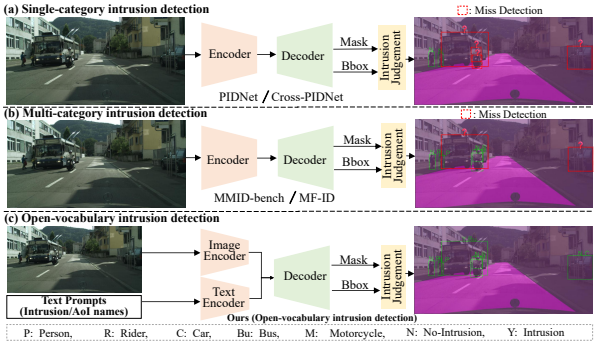

Figure 1: **Workflow comparisons** of different intrusion detection methods. Here, (a), (b), and (c) denote the Single-category, Multi-category, and proposed Open-vocabulary intrusion detection paradigms, respectively. '?' denotes the missed detection (False Negative). We can find that previous works can only detect the predefined intrusion category; our framework can detect more categories correctly, which demonstrates the validity of our paradigm.

To accomplish the above OVID task, the greatest difficulty is that there is still a lack of relevant datasets. Currently, some promising datasets, *e.g.*, ImageNet (Deng et al., 2009), COCO (Lin et al., 2014) and specific autonomous driving datasets, *e.g.*, Cityscapes (Cordts et al., 2016b), BDD100K (Yu et al., 2020) are proposed. These datasets are not suitable for our intrusion detection task due to the lack of intrusion labels. Fortunately, in recent works, some encouraging intrusion detection datasets have been proposed, *e.g.*, Cityintrusion (Sun et al., 2020), Cityintrusion-Multicategory (Han et al., 2024b), and Multi-Domain Multi-Category Datasets (Han et al., 2024c). These datasets provide multi-category, multi-domain and intrusion labels ('**N**'/'**Y**'), *i.e.*, '**N**' and '**Y**'denotes No-intrusion and Intrusion. Although these datasets contain multiple categories and domains, they can not meet the requirements of the OVID task. On one hand, these datasets still lack lots of common intrusion categories, *e.g.*, Car, Bus, Truck. On the other hand, these datasets solely contain image labels without matching text labels, which impairs their practicality in open-world intrusion detection where the model is required to generalize to new, unseen objects. To this end, we propose an extensive and comprehensive intrusion detection dataset, Cityintrusion-OpenV, for the OVID task.

The second difficulty is that there is still a lack of an effective and efficient open-vocabulary intrusion detection framework. Although some promising multi-task intrusion detection frameworks (Sun et al., 2020; Han et al., 2024b) and open-vocabulary detectors are proposed (Kim et al., 2023; Yao et al., 2023), these detectors still can not meet the requirements of the OVID task. The main reason is that the former is constrained by limited detection categories, and the latter can only perform a detection task. Inspired by promising works (Han et al., 2024b), we propose an *effective*, *multi-modal*, *multi-task*, and *end-to-end* open vocabulary intrusion detection framework, OVIDNet, to accomplish the task. The input of OVIDNet contains two different modalities, images and text. Subsequently, these inputs are sent to encoders to extract features, then decoded and predicted using the decoder. In the decoder, two simple yet effective strategies are designed to boost the performance of OVIDNet: 1) A Multi-Distributed Noise Mixing strategy is introduced to enhance the location information of unknown and unseen categories. 2) A Dynamic Memory-Gated module is designed to capture the contextual information in complex scenarios. Finally, the intrusion detection results are determined jointly by the upper and lower branches.

In summary, our contributions are as follows: **(1) Novel task and dataset.** To the best of our knowledge, the task of dynamic-view **O**pen **V**ocabulary **I**ntrusion **D**etection is proposed for the first time. This is the first multi-modal try in the vision-based intrusion task. A new benchmark, including a dataset called Cityintrusion-OpenV, and some strong baselines, is given for this task. **(2) Effective design and strategy.** An effective, multi-modal, multi-task, and end-to-end framework, OVIDNet, is designed as a strong baseline for this new benchmark. Besides, two effective strategies are proposed to improve the generalization and performance of the framework, including the Multi-Distributed Noise Mixing Strategy and the Dynamic Memory-Gated module. **(3) Adequate experiments and strong results.** Comprehensive experiments and comparisons are conducted to verify the effectiveness of the proposed framework and methods. The results show that our framework not only reaches the current SOTA level but also maintains strong high practicality with task-specific transfer and zero-shot prediction abilities.

2 Related Works

Traditional Vision-based Intrusion Detection. Intrusion detection can be divided into static and dynamic intrusion detection. Static intrusion detection has been explored in detail due to its simplicity, *e.g.*, Adaptive Background Subtraction (Stauffer & Grimson, 2000), Histogram of Oriented Gradients (Zhang et al., 2015). However, static intrusion detection does not meet the requirements of dynamic intrusion detection. The primary reason is that images captured by cameras can change at any time, which imposes higher real-time and accuracy requirements. Fortunately, with the rapid development of computer vision, some promising works are proposed to solve the dynamic-view intrusion detection, *e.g.*, PIDNet (Sun et al., 2020), Cross-PIDNet (Shi et al., 2022). However, the practice of these works is limited due to the **single category** of intrusion. To compensate for the limitations, some encouraging works are designed to border the intrusion category, *e.g.*, MF-ID (Han et al., 2024b), MMID-bench (Han et al., 2024c). Although intrusion detection has expanded significantly, the intrusion category remains fixed and single, which seriously hinders the practicality in the real world. To address these, we propose an open vocabulary intrusion detection task (OVID) for the first time, to solve the problem with limited intrusion categories and improve its practicality.

Open-Vocabulary Detection. Open-vocabulary detection (**OVD**) aims to detect unseen classes in the training stage in a zero-shot manner. Some promising open vocabulary detectors are designed to solve the OVD task, *e.g.*, Grounding DINO (Liu et al., 2023), YOLO-world (Cheng et al., 2024), and achieve excellent performance on real-world detection tasks. However, these OVD works are not suitable for our intrusion detection task. A major reason is that our OVID task is a multi-task with detection and segmentation simultaneously, not only a single detection task. OpenSeeD (Zhang et al., 2023) proposes a new framework for joint detection and segmentation, but this framework cannot meet the requirements of our OVID task due to a lack of intrusion judgment capability. For this reason, we propose a new framework, OVIDNet, to meet the needs of our OVID task.

3 Systematic Datasets

To compensate for the lack of richness in the categories of intrusion detection datasets, we develop an Open-Vocabulary Intrusion Detection dataset, namely **Cityintrusion-OpenV**, for the first time. The detailed automatic generation method of the proposed datasets is presented in **Appendix A.1**. Our new dataset is established on the promising Cityscape (Cordts et al., 2016b). Inspired by promising work MMID-bench (Han et al., 2024c), our new dataset also contains multi-categories and multi-domains. Differently, proposed datasets have more intrusion categories, not 4 categories in Multi-Domain Multi-Category datasets, but all potential/possible **8** intrusion categories in the cityscape dataset. Following some promising works (Han et al., 2024c), the detail Intrusion('**Y**')/No-intrusion('**N**') labels are provided by Automated Label Processes. And the judgment threshold is also set to **20**. To demonstrate the superiority of our dataset, we first present some visualization comparison, as shown in Figure 2. We can observe that our datasets provide the correct intrusion and no-intrusion labels and have richer categories of intrusions.

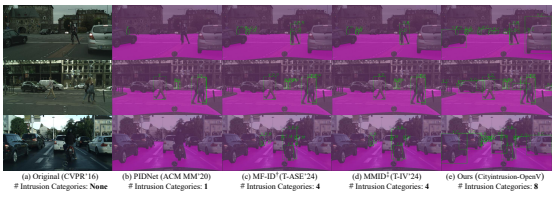

Figure 2: The visualization comparison between our datasets and other promising intrusion detection datasets. † and ‡ denote fine-grained and multiple domains, respectively.

Then, we compare the quantitative results between the proposed Cityintrusion-OpenV and other promising intrusion detection datasets, as shown in Table 1. We can find that our dataset contains more intrusion categories and has more sufficient 'Y'/'N' cases per image (**18.03** cases per image in the whole dataset), which significantly improves the intrusion detection dataset richness (about **2**× up compared to others). More detailed information, data statistics, and more visualization comparisons are presented in **Appendix A**.

Table 1: The comparison between previous intrusion detection datasets and our datasets. † denotes multiple domains.

Intrusion Detection Dataset Names	Categories	'Y'/'N' Cases	Cases per image
Cityintrusion (Sun et al., 2020; Shi et al., 2022)	1	4599/15084	7.3
Cityintrusion-Multicategory (Han et al., 2024b)	4	5431/22683	9.59
Multi-Domain Multi-Category (Han et al., 2024c;a)	4	5431/22683†	9.59
Ours (Cityintrusion-OpenV)	8	24750/37899	**18.03**

4 THE PROPOSED FRAMEWORK AND METHODS

4.1 PRELIMINARY

In the proposed OVID task, given a specific object detection dataset $\mathbf{D}^d$, $\mathbf{D}^d = \left\{\left(\mathbf{I}_i^d, \mathbf{M}_i^d\right)\right\}_{i=1}^{|\mathbf{D}^d|}$ and segmentation dataset $\mathbf{D}^s$, $\mathbf{D}^s = \{(\mathbf{I}_i^s, \mathbf{M}_i^s)\}_{i=1}^{|\mathbf{D}^s|}$, where $\mathbf{I}_i^d$ and $\mathbf{I}_i^s$ denotes the detection and segmentation samples, $\mathbf{M}_i^d$, $\mathbf{M}_i^s$ denotes the corresponding labels. For $\mathbf{M}_i^d$, we usually use four bounding box labels (b) and a category label (c^d) to express it, $b \in \mathbb{R}^4$, $c^d \in \mathcal{C}^d$. $\mathcal{C}^d$ denotes the category space of detection dataset ($\mathbf{D}^d$). For $\mathbf{M}_i^s$, we usually use fine labeling (assigning a category c^s to each pixel in the sample $\mathbf{I}_i^s$), $c^s \in \mathcal{C}^s$, $\mathcal{C}^s$ denotes the category space of segmentation dataset ($\mathbf{D}^s$). Besides, we divide the detection and segmentation dataset into ($\mathbf{D}_T^d$, $\mathbf{D}_T^s$), ($\mathbf{D}_V^d$, $\mathbf{D}_V^s$). $\mathbf{D}_T^d$, $\mathbf{D}_V^d$ denotes the training and validation of detection dataset. $\mathbf{D}_T^s$, $\mathbf{D}_V^s$ denotes the training and validation of segmentation dataset. Following the Open-Vocabulary detection and segmentation paradigms, we can express the training and validation category as $\mathbf{C}_T^d$ and $\mathbf{C}_V^d$, where $\mathbf{C}_T^d$ is base categories and $\mathbf{C}_T^d \in \mathbf{C}_V^d$. The category space of the new categories in $\mathbf{C}_V^d$ are named as $\mathcal{C}^N$, and $\mathcal{C}^N = \mathbf{C}_V^d \setminus \mathbf{C}_T^d \neq \varnothing$. The same is true for the segmentation dataset. For $\mathbf{I}_i$, we use the text Encoder ($\mathbf{E}^\mathbf{T}$) to convert text information into text embeddings, *i.e.*, $\mathbf{F}^\mathbf{T} = \mathbf{E}^\mathbf{T}(\mathbf{Text})$ and use the image Encoder ($\mathbf{E}^\mathbf{I}$) to extra the image feature, *i.e.*,$\mathbf{F}^\mathbf{I} = \mathbf{E}^\mathbf{I}(\mathbf{Img})$. All features are sent to a Decoder ($\mathbf{D}$) for decoding. Finally, the segmentation AoI and bonding box are extracted to calculate the intrusion results and express it as

$$\mathbf{I}_s = \mathbf{J}\left\{\mathbf{D}\left(\mathbf{F}^\mathbf{T}, \mathbf{F}^\mathbf{I}\right) \xrightarrow{\mathbf{e}} \left(\mathbf{Box}^\mathrm{p}, \mathbf{Aoi}^\mathrm{p}\right)\right\}, \tag{1}$$

where $\mathbf{I}_s$ denotes the final intrusion results. $\mathbf{J}$ denotes the intrusion judgment module. $\xrightarrow{e}$ denotes the extract two key information from the Decoder ($\mathbf{D}$). $\mathbf{Box}^\mathrm{p}$, $\mathbf{Aoi}^\mathrm{p}$ denote the prediction of the bounding box and AoI, respectively.

4.2 OVERALL FRAMEWORK

In this section, we introduce the proposed OVIDNet, as shown in Figure 3. We improve the original OpenSeeD (Zhang et al., 2023) to make it more suitable for our OVID task. Firstly, we use two different encoders, text and image encoders, to extract features for text prompts and images. The features are sent to the decoder. In the decoder, we design two effect methods to improve the generalization of the proposed framework: Multi-Distributed Noise Mixing and Dynamic Memory-Gated Module, respectively. Finally, we extract detection results and the segmentation results in the decoder to calculate the overlapping pixel values and determine whether it constitutes an intrusion. Once the overlapping pixel value exceeds a certain threshold (t), a warning ('Y/N, Class') will be added to the detected intruder surround box. Note that 'Y', 'N', and 'Class' denote the Intrusion, Non-intrusion, and Class name. (Here, class abbreviations are used instead of complete labels to easily show our results. The detailed correspondence between the two is shown in **Appendix A.4**.)

4.3 MULTI-DISTRIBUTED NOISE MIXING STRATEGY

In the original OpenSeeD model, noise generation methods usually use a uniform noise distribution and a fixed percentage of noise dynamics, as shown in Equation 2.

$$\mathbf{B}_f = \mathbf{C}\left\{\mathbf{B}_e + \mathbf{N}_r \odot \Delta \odot \Upsilon,\ \mathbf{0},\ \mathbf{1}\right\}, \tag{2}$$

where $\mathbf{B}_e$ denotes the set of the bounding box, $\mathbf{B}_e$ can be expressed by center point ($\mathbf{x}$, $\mathbf{y}$) and width, height ($\mathbf{w}$, $\mathbf{h}$). Δ denotes the range of the disturbance and $\Delta = \left\{\frac{\mathbf{w}}{2}, \frac{\mathbf{h}}{2}, \mathbf{w}, \mathbf{h}\right\}$. Υ is a constant noise scaling factor. $\mathbf{N}_r$ denotes the random distribution and $\mathbf{N}_r \sim \mathcal{U}(-1, 1)$. $\odot$ denotes the element-wise product. $\mathbf{C}$ denotes that all value is clamped between $\mathbf{0}$ and $\mathbf{1}$. However, in the real world, this method can not adapt to dynamic environments and scenarios, *e.g.*, different sizes and changing objects, and challenging intrusion scenarios. Therefore, to address this issue, we propose a new **M**ulti-**D**istributed **N**oise **M**ixing Strategy, as shown in Equation 3. The idea of the proposed Multi-Distributed Noise Mixing Strategy is very simple yet effective. When confronted with complex dynamic environments, models need to cope with the variations of different targets and scenarios.

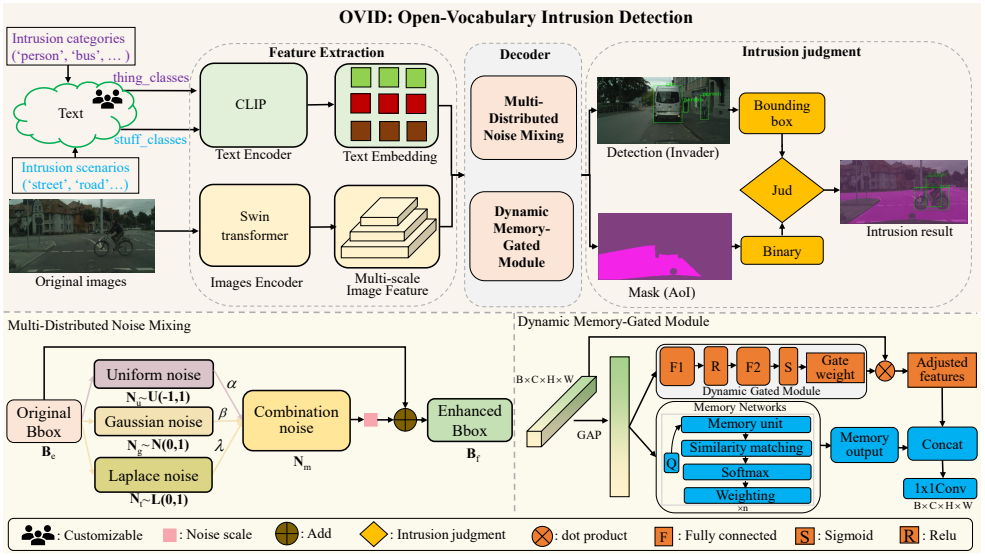

Figure 3: The overall framework and pipeline of our proposed OVIDNet. The input of OVIDNet consists of two different modalities: Text and Images. The text includes some customizable and common intrusion categories and scenarios. The image denotes the corresponding original images. Then, the text and images are sent to different encoders to extract features. These features will be sent to the decoder for decoding and prediction. In the encoder, we design a multi-distributed noise mixing strategy and a dynamic memory-gated module to enhance generalization in open scenarios. Finally, we extract the predicted bounding box and predicted AoI mask to calculate the overlapping pixels and give the final intrusion results. Once the overlapping pixels are greater than the threshold (t), it will be judged as an intrusion. Otherwise, it will be judged as no-intrusion.

Specifically, for tiny objects, fine-grained perturbations are used to preserve their detailed features. Meanwhile, large-scale perturbations to strengthen the global features for large objects.

$$\mathbf{B}_f = \mathbf{C}\left\{\mathbf{B}_e + (\alpha \cdot \mathbf{N}_u + \beta \cdot \mathbf{N}_g + \gamma \cdot \mathbf{N}_t) \odot \Delta \odot \Theta,\ \mathbf{0},\ \mathbf{1}\right\}, \tag{3}$$

where $\mathbf{N}_u \sim \mathcal{U}(-1,1)$, $\mathbf{N}_g \sim \mathcal{N}(0,1)$ and $\mathbf{N}_t \sim \mathcal{L}(0,1)$. $\mathcal{L}$ denotes the Laplace distribution. α, β and γ is the coefficient of $\mathcal{U}$, $\mathcal{N}$, and $\mathcal{L}$ distributions, respectively. Note that $\alpha + \beta + \gamma = 1$. Θ denotes the proposed dynamic varying noise ratio based on the detection area of the bounding box, and $\Theta = \tau \cdot (1 + \log(1 + \mathbf{A}))$. $\mathbf{A}$ denotes the area of the bounding box and $\mathbf{a} = \mathbf{w} \cdot \mathbf{h}$. Besides, $\mathbf{C}$ and Δ are defined as the same as the Equation 2. Our detailed algorithm is shown in Algorithm 1.

4.4 Dynamic Memory-Gated Module

To address the challenges of insufficient long-term dependency modeling and poor dynamic scene adaptation in our OVID task, we propose a Dynamic Memory-Gated Module. Given a input feature $\mathbf{X} \in \mathbb{R}^{\mathcal{B}\times\mathcal{C}\times\mathcal{H}\times\mathcal{W}}$, we first use global average pooling (GAP) to extract a global context query vector ($\mathbf{Q} \in \mathbb{R}^{\mathcal{B}\times\mathcal{C}}$), express it as $\mathbf{Q} = \text{GAP}(\mathbf{X})$, where $\mathbf{B}$, $\mathbf{C}$, $\mathbf{H}$ and $\mathbf{W}$ denotes the batch_size, channel, height and width. Then, we introduce a dynamic memory retrieval module and express it as

$$\mathbf{O}_m = \text{softmax}\left(\frac{\mathbf{Q}\mathbf{M}_K^{\mathbf{T}}}{\sqrt{d}}\right)\mathbf{M}_V, \tag{4}$$

where $\mathbf{Q} \in \mathbb{R}^{\mathcal{B}\times\mathcal{C}}$ denotes query vector. $\mathbf{M}_K \in \mathbb{R}^{\mathcal{B}\times\mathcal{C}}$ denotes the memory key, and $\mathbf{M}$ is the number of memory units. $\mathbf{M}_V \in \mathbb{R}^{\mathcal{M}\times\mathcal{C}}$ denotes the memory value, and $\mathbf{M}_V$ is used to store the feature information corresponding to the key. $\mathbf{O}_m \in \mathbb{R}^{\mathcal{B}\times\mathcal{C}}$ denotes the memory output by retrieving. Finally, retrieved memory output ($\mathbf{O}_m$) and input features ($\mathbf{X}$) are fused by concatenation and 1×1 Conv. We can express it as

$$\mathbf{X}_f = \text{Conv1x1}(\text{Concat}(\mathbf{X} \odot \mathbf{W}), \mathbf{O}_m), \tag{5}$$

where $\mathbf{X}_f$ denotes the fusion feature. $\mathbf{W}$ denotes the generate dynamic weights and $\mathbf{W} = \sigma(\mathbf{W}_2\text{ReLU}(\mathbf{W}_1 Q))$. $\mathbf{W}_1, \mathbf{W}_2$ denotes the weight of fully connected networks. $\mathbf{W}_1 \in \mathbb{R}^{\mathcal{C}\times d}$, $\mathbf{W}_2 \in \mathbb{R}^{d\times\mathcal{C}}$. σ denotes the sigmoid function.

Algorithm 1 **M**ulti-**D**istributed **N**oise **M**ixing Strategy

Require: Bounding box parameters $\mathbf{B}_e$, Noise scale τ; Uniform noise weight α, Gaussian noise weight β, Laplace noise weight γ
Ensure: Augmented bounding box parameters $\mathbf{B}_f$.
$\triangleright$ $\mathbf{D}$ is a tensor of the same shape as $\mathbf{B}_e$
Initialize $\mathbf{D} \leftarrow \mathbf{0}$
$\triangleright$ Compute the area of each bounding box
$\mathbf{A} \leftarrow \mathbf{B}_e[:, 2] \cdot \mathbf{B}_e[:, 3]$.
$\triangleright$ Compute dynamic noise scale for each box
$\mathbf{\Theta} \leftarrow \tau \cdot (1 + \log(1 + \mathbf{A}))$
$\triangleright$Define perturbation directions for center and size
$\mathbf{\Delta}[:, : 2] \leftarrow \mathbf{B}_e[:, 2 :]/2$ # Perturb center
$\mathbf{\Delta}[:, 2 :] \leftarrow \mathbf{B}_e[:, 2 :]$ # Perturb width and height
$\triangleright$ Generate noise from multiple distributions
$\mathbf{N}_u \sim \mathcal{U}(-1, 1)$, $\mathbf{N}_g \sim \mathcal{N}(0, 1)$ and $\mathbf{N}_t \sim \mathcal{L}(0, 1)$
$\triangleright$ Compute the weighted combination of noise
$\mathbf{N}_{\mathrm{m}} \leftarrow \alpha \cdot \mathbf{N}_u + \beta \cdot \mathbf{N}_g + \gamma \cdot \mathbf{N}_l$
$\triangleright$ Add scaled noise to bounding box parameters
$\mathbf{B}_f \leftarrow \mathbf{B}_e + (\mathbf{N}_{\mathrm{m}} \odot \mathbf{\Delta} \odot \mathbf{\Theta})$
$\triangleright$ Clamp augmented bounding boxes to the valid range
$\mathbf{B}_f \leftarrow \mathrm{Clamp}(\mathbf{B}_f, \mathbf{0}, \mathbf{1})$
return $\mathbf{B}_f$

5 Experiments And Analyses

5.1 Experimental Settings

Implementation Details. We conduct all experiments on a computer with 8 NVIDIA GeForce RTX 2080Ti GPUs. Unless specified, the Max_Iter, Batch_size_total, CHECKPOINT_PERIOD, EVAL_PERIOD of all experiments are set to 15000, 8, 15000, and 15000, respectively. The image encoder and text encoder adopt tiny-swin-transformer (Liu et al., 2021) and Clip (Radford et al., 2021), respectively. More hyperparameter details can be found in **Appendix B**.

Datasets. Our experiments are conducted in some publiy datasets, *e.g.*, COCO (Lin et al., 2014), Citytscape (Cordts et al., 2016a), Foggy-Cityscape (Sakaridis et al., 2018) and Cityintrusion-OpenV. In addition, to provide more visualization results, we also test and report visualization demo results on other datasets, *e.g.*, the ShanghaiTech Campus dataset (Luo et al., 2017), and the UA-DETRAC (Wen et al., 2020). Note that in our experiment, we adopt two manners, *i.e.*, zero-shot and task-specific transfer, to evaluate the performance of the model.

Metrics. In order to report the quantitative results of our experiments more comprehensively, inspired by some previous promising work (Han et al., 2024c;b), the mIOU(%) and mAP(%) are utilized to evaluate the sub-task performance of segmentation and object detection. For the intrusion detection performance, we also use three different intrusion detection metrics: AccY(%), AccN(%), and Acc(%) to quantify. Besides, some additional metrics, *e.g.*, panoptic segmentation metrics, PQ(%), SQ(%), RQ(%), and every AP(%), AP@.5(%) of intrusion categories, are reported to evaluate the zero-shot performance of the model.

Baseline/Comparison Models. We compare with the OpenSeeD (Zhang et al., 2023) model because of its multi-task capability and its promising performance in open-vocabulary tasks. The multi-task feature is consistent with our task. Besides, we also compare the latest and promising intrusion works, *e.g.*, PIDNet (Sun et al., 2020), Cross-PIDNet (Shi et al., 2022), MMID-bench (Han et al., 2024c), MF-ID (Han et al., 2024b).

5.2 Main Results

Compared with promising open-vocabulary works. We first compare the multiple performances with the promising OpenSeeD model and report three zero-shot detection performances, *i.e.*, PQ(%),

SQ(%), RQ(%), and three task-specific transfer intrusion performances, *i.e.*, AccY(%), AccN(%), Acc(%), as shown in Table 2. We can find that in different tasks, for the panoptic segmentation performance (PQ), compared with OpenSeeD, our methods can improve it by 2.19% and 1.12%, respectively. Besides, for intrusion detection performance (Acc), our model can surpass it by 3.43% and 3.45%, respectively, which verifies the effectiveness of the proposed model and strategies.

Table 2: The Zero-shot and Task-specific transfer comparison results between promising multi-task open-vocabulary and proposed OVIDNet framework in different datasets.

-	Zero-shot Detection (Panoptic segmentation)				Task-specific Transfer (Intrusion detection)			
Model	Test data 1	RQ(%)	SQ(%)	PQ(%)	Test data 2	AccY(%)	AccN(%)	Acc(%)
OpenSeeD	Cityscape	18.22	43.68	14.03	Ours (Normal)	18.72	36.19	29.36
	Foggy-Cityscape	18.07	36.71	14.28	Ours (Foggy)	22.04	25.88	24.38
OVIDNet (Ours)	Cityscape	20.36	36.17	**16.22**	Ours (Normal)	24.43	38.16	**32.79**
	Foggy-Cityscape	19.05	33.71	**15.40**	Ours (Foggy)	27.72	27.90	**27.83**

Compared with promising intrusion detection works. We also compare some intrusion detection works, as shown in Table 3. We can see that, compared with previous intrusion works, our model not only has an open structure but also detects more intrusion categories. More importantly, our model has strong generalization capability and achieves zero-shot detection, which is not only pre-trained/pre-undefined categories. In addition, we can observe that as the task difficulty increases, *i.e.*, common intrusion detection task (PIDNet, Cross-PIDNet, MF-ID)→domain adaptation intrusion detection task (MMID-bench)→Open-vocabulary intrusion detection task (OVID), the performance of each category continuously decreases. The main reason is that, as the difficulty of different intrusion detection tasks increases, the requirements of different intrusion detection frameworks are also raised in the open world, especially their generalization and zero-shot capabilities.

Table 3: The comparison between our work and promising intrusion detection works. Here, 'close' and 'open' denote the different detection structures, respectively. 'ZSD' denotes Zero-shot detection. ✓and ✗denote the intrusion category as assessable or not assessable, respectively. † denotes that the backbone is BNet.

Method	Venue	Structure	ZSD	P(%)	R(%)	M(%)	Bc(%)	Tk(%)	Bu(%)	Tn(%)	C(%)
PIDNet (Sun et al., 2020)	ACM MM'20	close	✗	67.1	✗	✗	✗	✗	✗	✗	✗
			✗	63.3†	✗	✗	✗	✗	✗	✗	✗
Cross-PIDNet (Shi et al., 2022)	T-IV'21	close	✗	74.7	✗	✗	✗	✗	✗	✗	✗
			✗	72.1†	✗	✗	✗	✗	✗	✗	✗
MF-ID (Han et al., 2024b)	T-ASE'24	close	✗	45.8	39.8	34.5	38.2	✗	✗	✗	✗
MMID-bench (Han et al., 2024c)	T-IV'24	close	✗	37.4	34.6	20.7	33.1	✗	✗	✗	✗
OVIDNet (Ours)	-	open	✓	28.6	0.0	27.8	36.5	32.9	45.4	13.6	47.0

Zero-shot and Task-specific transfer evaluation results on proposed strategies. We then test the zero-shot/task-specific transfer performance of the proposed strategies. Specifically, we train our model on the COCO dataset and validate it on the Cityscape datasets to obtain the segmentation and detection performance in a zero-shot manner. Besides, we also test the intrusion detection performance on the proposed Cityintrusion-OpenV datasets by a task-specific transfer manner, as shown in Table 4. **B** denotes the baseline. We can observe that as different strategies are added, multiple performances are improved, not only intrusion detection but also zero-shot performance, *e.g.*, PQ(%) and mIOU(%). Compared with the baseline, the intrusion performance (Acc) can surpass it by 3.43%. In addition, the zero-shot performance can surpass it by 2.19% (PQ) and 1.1% (mIOU), respectively. More detailed results can be found in **Appendix C.1**.

Table 4: Zero-shot and Task-specific transfer quantitative results of the proposed different strategies.

B	DMG	MDNM	PQ(%)	mIOU(%)	mAP@.5(%)	AccY(%)	AccN(%)	Acc(%)
✓	✗	✗	14.03	28.34	27.58	18.72	36.19	29.36
✓	✓	✗	15.80	28.78	29.16	20.06	37.56	30.72
✓	✗	✓	15.33	29.40	28.56	21.01	38.64	31.75
✓	✓	✓	16.22	29.37	28.98	24.43	38.16	**32.79**

Generalization Verification in cross-domain tasks. We further test the performance of our OVIDNet framework and strategies in cross-adverse weather tasks, *e.g.*, Normal→Foggy, to verify generalization capabilities. Note that all performance results are given by the pre-trained (in Normal weather) and inference (in adverse weather) manners, as shown in Figure 4. We can find that our OVIDNet is effective even in adverse weather and exhibits promising intrusion performance. Under

three different foggy coefficient setting, *i.e.*, $\alpha = 0.005$, $\alpha = 0.01$, $\alpha = 0.02$, our OVIDNet can surpass the baseline model by 2.96%, 3.22%, and 3.45%, respectively. Besides, our strategies can also improve the zero-shot performance under cross-domain tasks, *e.g.*, compared with the baseline of three different foggy coefficient settings, the PQ(%) in the Normal→Foggy tasks can surpass them by 1.29%, 1.21%, and 1.12%, respectively. More details results can be found in **Appendix C.2**.

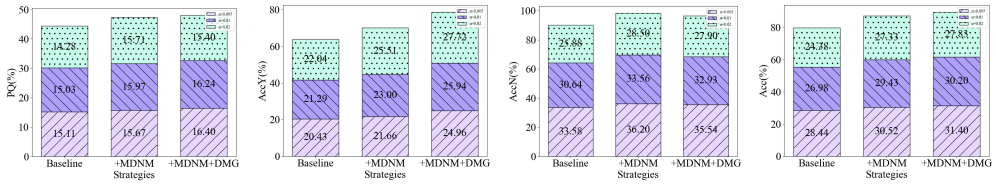

Figure 4: Generalization Verification in cross-domain tasks.

Visualization Comparisons. We also present some visualization comparison results to verify the zero-shot performance and effectiveness of the proposed framework and methods, as shown in Figure 5. We can find that our framework can present promising visualization detection results, not only detecting intrusion behaviors correctly but also giving correct Intrusion ('Y')/No-intrusion ('N') labels, which proves the effectiveness of our framework and approach. Note that our OVIDNet can improve the zero-shot segmentation performance of AoI; in this case, the AoI is the road. More visualization comparison results are presented in **Appendix C.3**.

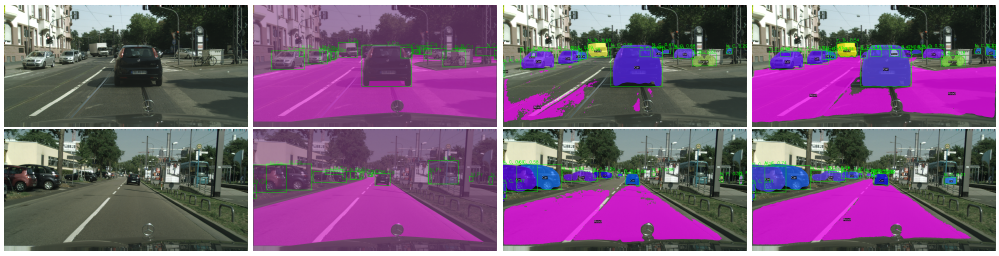

(a) Original Images (b) Ground Truth (c) Baseline (d) Ours

Figure 5: The visualization comparison results.

5.3 Ablation Experiments

Multi-Distributed Noise Mixing Strategy. We analyze the proposed multi-distributed noise mixing strategy and conduct extra ablation experiments to verify its effectiveness. The detailed results are shown in Table 5. We can find that when the α=**0.5**, β=**0.1**, γ=**0.4**, the intrusion detection performance can reach the best, with a 31.75% intrusion accuracy. The main reason is that, in task-specific transfer, the model focuses more on texture features and spatial perturbations. Besides, the transfer task is performed during normal weather. Thus, the need for weather changes and light perturbations is low. In this paper, we set the α, β, γ to **0.5**, **0.1** and **0.4**, respectively.

Dynamic Memory-Gated Module. We also explore the effect of different memory unit sizes on intrusion detection performance, as shown in Table 5. IOU^r denotes the zero-shot segmentation results of the road. We can see that the best intrusion performance can be reached when **M=40**. The main reason is that the larger memory can help capture richer history and global features, especially in open-world intrusion detection. However, larger memory units also introduce more irrelevant information, making it difficult to focus on key memory features. Conversely, fewer memory units can help the model focus on features relevant to intrusion detection, but if the memory units are too low, it will lead to a loss of diversity and complexity required

Table 5: The ablation experiments of the proposed strategies. **B** denotes the baseline.

Ablation 1: Multi-Distributed Noise Mixing Strategy							
Methods				Metrics			
B	# $\mathcal{U}(\alpha)$	# $\mathcal{N}(\beta)$	# $\mathcal{L}$ (γ)	PQ	IOU^r(%)	mAP(%)	Acc(%)
✓	✓(1)	✗	✗	14.03	74.1	27.6	29.36
✓	✓(0.5)	✓(0.4)	✓(0.1)	14.37	70.1	32.1	30.28
✓	✓(0.5)	✓(0.2)	✓(0.3)	14.78	68.8	25.8	30.48
✓	✓(0.5)	✓(0.3)	✓(0.2)	14.53	78.5	25.9	31.03
✓	✓(0.5)	✓(0.1)	✓(0.4)	15.33	74.6	28.6	**31.75**
Ablation 2: Dynamic Memory-Gated Module							
Methods				Metrics			
B	Memeroy units			PQ	IOU^r(%)	mAP(%)	Acc(%)
✓	✗			14.03	74.1	27.6	29.36
✓	✓(M=30)			14.84	76.0	27.5	30.31
✓	✓(M=40)			15.80	76.5	29.5	**30.72**
✓	✓(M=50)			13.03	83.5	27.1	28.42

for the intrusion task, affecting the understanding of complex intrusion scenarios. In this paper, we set the memory units to **40**.

5.4 More Insightful and Interesting Experiments

Experiment 1: Why is the performance result of category 'Rider' is '0.0' in the Table 3? To answer this question, 1) we first investigate some of the latest open-vocabulary works (Bianchi et al., 2024; Ma et al., 2024). Some works denote that the understanding of fine-grained properties of objects and their parts is important. From this view, we conduct some experiments and provide the visualization comparison, as shown in Figure 6. We can find that our model recognizes the category 'Rider' as the category 'Person'. The main reason is that these two categories have similar features. 2) Besides, in the training dataset, the number of category 'Person' is much larger than the category 'Rider,' which leads to category imbalance. Therefore, these two factors will make it difficult to recognize the fine-grained category 'Rider'. In the future, we will explore more effective ways to compensate for these two limitations.

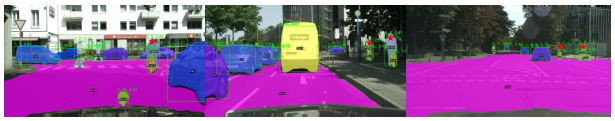

Figure 6: Some cases of recognizing 'Rider (R)' as 'Person (P)'. ★ denotes the detailed case locations.

Experiment 2: Real-scenario application exploration. To verify the high generality and universal applicability of our framework, we also provide some visualization results under different static scenarios, *e.g.*, intelligent monitoring, and security. Since static scenarios lack relevant intrusion detection datasets and labels, the specific quantitative evaluation results cannot be measured and given. However, inspired by some super-resolution works (Gandikota & Chandramouli, 2024; Korkmaz et al., 2024), we can report some demo visualization results. Here, we directly use our framework to infer public static scene datasets without any retraining process, *e.g.*, the ShanghaiTech Campus dataset (Luo et al., 2017), and the UA-DETRAC (Wen et al., 2020). Note that for different scenarios and intrusion categories, the number of text prompts can be customized. In our paper, we report multiple visualization results with different customizable text prompts . Besides, we use different domains, *e.g.*, Normal, Rainy, and Night, to evaluate the model's generalization performance, as shown in Figure 7. We can observe that our framework can detect and judge intrusion behavior, demonstrating the practicality and effectiveness of the proposed framework.

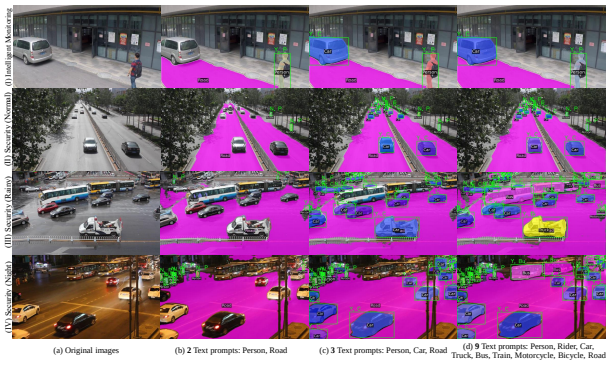

Figure 7: The visualization demo results in real scenarios. We directly utilize our framework to infer public static scenario datasets without any retraining process. We give three different text prompts customizable results, *i.e.*, 2 text prompts, 3 text prompts, and 9 text prompts, respectively.

6 Conclusion

In this paper, we propose a new and vital intrusion detection task, Open-Vocabulary Intrusion Detection (OVID). This is the first multi-modal attempt in the vision-based intrusion detection task. A new benchmark, including a relative dataset, an efficient multi-modal framework, and some strong baselines, is given for the specific task. Besides, two effective strategies are proposed to improve the generalization and enhance the performance of intrusion detection task in open scenarios, *i.e.*, the Multi-Distributed Noise Mixing and the Dynamic Memory-Gated module. Finally, rich experiments and comparisons are done to demonstrate the effectiveness of the proposed framework and strategies. In the future, we will further explore more useful methods to improve performance.

REFERENCES

Lorenzo Bianchi, Fabio Carrara, Nicola Messina, Claudio Gennaro, and Fabrizio Falchi. The devil is in the fine-grained details: Evaluating open-vocabulary object detectors for fine-grained understanding. In *Proceedings of the IEEE/CVF Conference on Computer Vision and Pattern Recognition*, pp. 22520–22529, 2024.

Liang-Chieh Chen, Yukun Zhu, George Papandreou, Florian Schroff, and Hartwig Adam. Encoder-decoder with atrous separable convolution for semantic image segmentation. In *Proceedings of the European conference on computer vision (ECCV)*, pp. 801–818, 2018.

Tianheng Cheng, Lin Song, Yixiao Ge, Wenyu Liu, Xinggang Wang, and Ying Shan. Yolo-world: Real-time open-vocabulary object detection. In *Proceedings of the IEEE/CVF Conference on Computer Vision and Pattern Recognition*, pp. 16901–16911, 2024.

Marius Cordts, Mohamed Omran, Sebastian Ramos, Timo Rehfeld, Markus Enzweiler, Rodrigo Benenson, Uwe Franke, Stefan Roth, and Bernt Schiele. The cityscapes dataset for semantic urban scene understanding. In *Proceedings of the IEEE conference on computer vision and pattern recognition*, pp. 3213–3223, 2016a.

Marius Cordts, Mohamed Omran, Sebastian Ramos, Timo Rehfeld, Markus Enzweiler, Rodrigo Benenson, Uwe Franke, Stefan Roth, and Bernt Schiele. The cityscapes dataset for semantic urban scene understanding. In *Proceedings of the IEEE/CVF International Conference on Computer Vision*, pp. 3213–3223, 2016b.

Jia Deng, Wei Dong, Richard Socher, Li-Jia Li, Kai Li, and Li Fei-Fei. Imagenet: A large-scale hierarchical image database. In *2009 IEEE conference on computer vision and pattern recognition*, pp. 248–255. Ieee, 2009.

Kanchana Vaishnavi Gandikota and Paramanand Chandramouli. Text-guided explorable image super-resolution. In *Proceedings of the IEEE/CVF Conference on Computer Vision and Pattern Recognition*, pp. 25900–25911, 2024.

Fujun Han, Peng Ye, Shukai Duan, and Lidan Wang. Ada-id: Active domain adaptation for intrusion detection. In *Proceedings of the 32nd ACM International Conference on Multimedia*, pp. 7404–7413, 2024a.

Fujun Han, Peng Ye, Ke Li, Shukai Duan, and Lidan Wang. Mf-id: A benchmark and approach for multi-category fine-grained intrusion detection. *IEEE Transactions on Automation Science and Engineering*, 2024b.

Fujun Han, Peng Ye, Chunyan She, Shukai Duan, Lidan Wang, and Derong Liu. Mmid-bench: A comprehensive benchmark for multi-domain multi-category intrusion detection. *IEEE Transactions on Intelligent Vehicles*, 2024c.

Dahun Kim, Anelia Angelova, and Weicheng Kuo. Region-aware pretraining for open-vocabulary object detection with vision transformers. In *Proceedings of the IEEE/CVF Conference on Computer Vision and Pattern Recognition*, pp. 11144–11154, 2023.

Alexander Kirillov, Eric Mintun, Nikhila Ravi, Hanzi Mao, Chloe Rolland, Laura Gustafson, Tete Xiao, Spencer Whitehead, Alexander C Berg, Wan-Yen Lo, et al. Segment anything. In *Proceedings of the IEEE/CVF International Conference on Computer Vision*, pp. 4015–4026, 2023.

Cansu Korkmaz, A Murat Tekalp, and Zafer Dogan. Training generative image super-resolution models by wavelet-domain losses enables better control of artifacts. In *Proceedings of the IEEE/CVF Conference on Computer Vision and Pattern Recognition*, pp. 5926–5936, 2024.

Tsung-Yi Lin, Michael Maire, Serge Belongie, James Hays, Pietro Perona, Deva Ramanan, Piotr Dollár, and C Lawrence Zitnick. Microsoft coco: Common objects in context. In *Computer Vision–ECCV 2014: 13th European Conference, Zurich, Switzerland, September 6-12, 2014, Proceedings, Part V 13*, pp. 740–755. Springer, 2014.

Shilong Liu, Zhaoyang Zeng, Tianhe Ren, Feng Li, Hao Zhang, Jie Yang, Chunyuan Li, Jianwei Yang, Hang Su, Jun Zhu, et al. Grounding dino: Marrying dino with grounded pre-training for open-set object detection. *arXiv preprint arXiv:2303.05499*, 2023.

Ze Liu, Yutong Lin, Yue Cao, Han Hu, Yixuan Wei, Zheng Zhang, Stephen Lin, and Baining Guo. Swin transformer: Hierarchical vision transformer using shifted windows. In *Proceedings of the IEEE/CVF international conference on computer vision*, pp. 10012–10022, 2021.

Weixin Luo, Wen Liu, and Shenghua Gao. A revisit of sparse coding based anomaly detection in stacked rnn framework. In *Proceedings of the IEEE International Conference on Computer Vision (ICCV)*, Oct 2017.

Yuqi Ma, Mengyin Liu, Chao Zhu, and Xu-Cheng Yin. Ha-fgovd: Highlighting fine-grained attributes via explicit linear composition for open-vocabulary object detection. *arXiv preprint arXiv:2409.16136*, 2024.

Dierck Matern, Alexandru Paul Condurache, and Alfred Mertins. Automated intrusion detection for video surveillance using conditional random fields. In *MVA*, pp. 298–301, 2013.

Alec Radford, Jong Wook Kim, Chris Hallacy, Aditya Ramesh, Gabriel Goh, Sandhini Agarwal, Girish Sastry, Amanda Askell, Pamela Mishkin, Jack Clark, et al. Learning transferable visual models from natural language supervision. In *International conference on machine learning*, pp. 8748–8763. PMLR, 2021.

Christos Sakaridis, Dengxin Dai, Simon Hecker, and Luc Van Gool. Model adaptation with synthetic and real data for semantic dense foggy scene understanding. In *Proceedings of the european conference on computer vision (ECCV)*, pp. 687–704, 2018.

Zhenyu Shi, Shibo He, Jingchen Sun, Tao Chen, Jiming Chen, and Hairong Dong. An efficient multi-task network for pedestrian intrusion detection. *IEEE Transactions on Intelligent Vehicles*, 8(1):649–660, 2022.

Chris Stauffer and W. Eric L. Grimson. Learning patterns of activity using real-time tracking. *IEEE Transactions on pattern analysis and machine intelligence*, 22(8):747–757, 2000.

Jingchen Sun, Jiming Chen, Tao Chen, Jiayuan Fan, and Shibo He. Pidnet: An efficient network for dynamic pedestrian intrusion detection. In *Proceedings of the 28th ACM International Conference on Multimedia*, pp. 718–726, 2020.

Chien-Yao Wang, Alexey Bochkovskiy, and Hong-Yuan Mark Liao. Yolov7: Trainable bag-of-freebies sets new state-of-the-art for real-time object detectors. In *Proceedings of the IEEE/CVF conference on computer vision and pattern recognition*, pp. 7464–7475, 2023.

Longyin Wen, Dawei Du, Zhaowei Cai, Zhen Lei, Ming-Ching Chang, Honggang Qi, Jongwoo Lim, Ming-Hsuan Yang, and Siwei Lyu. Ua-detrac: A new benchmark and protocol for multi-object detection and tracking. *Computer Vision and Image Understanding*, 193:102907, 2020.

Yunyang Xiong, Bala Varadarajan, Lemeng Wu, Xiaoyu Xiang, Fanyi Xiao, Chenchen Zhu, Xiaoliang Dai, Dilin Wang, Fei Sun, Forrest Iandola, et al. Efficientsam: Leveraged masked image pretraining for efficient segment anything. In *Proceedings of the IEEE/CVF Conference on Computer Vision and Pattern Recognition*, pp. 16111–16121, 2024.

Lewei Yao, Jianhua Han, Xiaodan Liang, Dan Xu, Wei Zhang, Zhenguo Li, and Hang Xu. Detclipv2: Scalable open-vocabulary object detection pre-training via word-region alignment. In *Proceedings of the IEEE/CVF Conference on Computer Vision and Pattern Recognition*, pp. 23497–23506, 2023.

Tao Ye, Xiao Cong, Yuliang Li, Zhikang Zheng, Xiangpeng Deng, Xiangming Yan, Xiaosong Li, and Xi Zhang. Few-shot railway intrusion detection without forgetting via double rpn and detector. *IEEE Transactions on Intelligent Vehicles*, pp. 1–16, 2024. doi: 10.1109/TIV.2024.3372776.

Fisher Yu, Haofeng Chen, Xin Wang, Wenqi Xian, Yingying Chen, Fangchen Liu, Vashisht Madhavan, and Trevor Darrell. Bdd100k: A diverse driving dataset for heterogeneous multitask learning. In *Proceedings of the IEEE/CVF conference on computer vision and pattern recognition*, pp. 2636–2645, 2020.

Hao Zhang, Feng Li, Xueyan Zou, Shilong Liu, Chunyuan Li, Jianwei Yang, and Lei Zhang. A simple framework for open-vocabulary segmentation and detection. In *Proceedings of the IEEE/CVF International Conference on Computer Vision*, pp. 1020–1031, 2023.

Yong-Liang Zhang, Zhi-Qin Zhang, Gang Xiao, Rui-Dong Wang, and Xia He. Perimeter intrusion detection based on intelligent video analysis. In *2015 15th International Conference on Control, Automation and Systems (ICCAS)*, pp. 1199–1204. IEEE, 2015.

Hengshuang Zhao, Jianping Shi, Xiaojuan Qi, Xiaogang Wang, and Jiaya Jia. Pyramid scene parsing network. In *Proceedings of the IEEE conference on computer vision and pattern recognition*, pp. 2881–2890, 2017.

Xu Zhao, Wenchao Ding, Yongqi An, Yinglong Du, Tao Yu, Min Li, Ming Tang, and Jinqiao Wang. Fast segment anything. *arXiv preprint arXiv:2306.12156*, 2023.

APPENDIX OVERVIEW

Table of contents:

A CITYINTRUSION-OPENV DATASET

In this subsection, we present additional information and details for the proposed Cityintrusion-OpenV dataset, including data statistics, visualization results, intrusion Dataset Comparisons, and the correspondence between full name, text prompt, abbreviation, and framework design motivation.

A.1 METHOD AND STATISTICS FOR PROPOSED DATASET

Automatic Generation Method. Inspired by promising intrusion detection works (Sun et al., 2020; Shi et al., 2022; Han et al., 2024b), our Cityintrusion-OpenV dataset is built based on the Cityscape dataset (Cordts et al., 2016a). The main reason is that the Cityscape datasets have segmentation and detection labels for the same original image, which provides a prerequisite for our multiple intrusion detection tasks. Additionally, following the relevant works (Han et al., 2024c), we also design an automatic labeling program to generate Intrusion ('Y') and No-intrusion ('N') labels. Note that the final intrusion detection overlapping pixel points are also set to **20** (Sun et al., 2020). The specific processes are shown as follows.

· **Step 1:** We first clean the original Cityscape (Cordts et al., 2016b)/Foggy-Cityscape (Sakaridis et al., 2018). After cleaning, we conduct frame alignment for these datasets. Note that a small number of objects that we don't care about or are incorrectly labeled will be removed in this process.

· **Step 2:** Based on the results in step 1, we can read the bounding box coordinates of the interested intrusion objects from the Cityscape/Foggy-Cityscape datasets. Additionally, we also read the area-of-interest (AoI) in the Cityscapes segmentation dataset (Cordts et al., 2016b).

· **Step 3:** For the obtained area-of-interest (AoI) in step 2, we binarize them with **0** and **1**.

· **Step 4:** After step 3, the bounding box coordinates from step 2 are projected into the binarized area-of-interest (AoI).

· **Step 5:** We calculate the overlapping pixel values between AoI and bounding box in step 4.

· **Step 6:** To get the final intrusion/no-intrusion labels: 'N/Y, Class', we compare overlapping pixel values in step 5 with a setting threshold, where 'N' denotes Non-Intrusion, 'Y' denotes Intrusion, and 'Class' denotes names of intrusion objects. Note that, following previous work Sun et al. (2020), the threshold is set to 20.

· **Step 7:** To obtain and present our final intrusion detection dataset better, we blended the segmented images containing the intrusion labels in step 6 with the original images in step 1.

· **Step 8:** Finally, to ensure the quality and accuracy of the proposed datasets, a team of three students are organized to manually inspect and verify the annotations.

Statistical Analysis. Then, we conduct a detailed statistical analysis, as shown in Table 6. We provide details of the number of intrusion and non-intrusion cases for each category in the training and validation sets of the dataset, along with the total average. We can observe that some intrusion categories reach an average of 9.16 (car) and 6.16 (person). The total average of the whole dataset can reach **18.03**, surpassing previous promising intrusion detection datasets greatly. Rich labels can meet the requirements and provide a data foundation for the proposed OVID task.

Table 6: The detailed statistics of proposed datasets. T and V denote the training and validation datasets, respectively. † denotes the average of the sum of each category in the training and validation. ‡ denotes the total average in the whole dataset.

Categories	Person	Rider	Car	Truck	Bus	Train	Motorcycle	Bicycle
	T|V	T|V	T|V	T|V	T|V	T|V	T|V	T|V
Intrusion cases ('Y')	3567|716	698|226	14545|2493	246|52	219|67	88|9	270|55	1138|361
Non-Intrusion cases ('N')	14427|2703	1109|330	12610|2174	243|41	166|31	83|14	469|94	2591|814
Total cases	17994|3419	1807|556	27155|4667	489|93	385|98	171|23	739|149	3729|1175
Average (Per very image)	6.05|6.84	0.61|1.11	9.13|9.33	0.16|0.19	0.13|0.20	0.06|0.05	0.25|0.30	1.25|2.35
Average†(Per very image)	6.16	0.68	9.16	0.17	0.14	0.06	0.26	1.41
Total average‡ (Per very image)	**18.03**							

A.2 More Visualization Results

In order to better present our proposed dataset, we also provide more visualization results, as shown in Figure 8. Different from the previous single category (President) (Sun et al., 2020; Shi et al., 2022) and four categories (President, Motorcycle, Rider, Bicycle) (Han et al., 2024b;c), we can find that our Cityintrusion-OpenV dataset contains multiple different intrusion categories, not only single or four categories. All possible intruder categories can be considered in our dataset, *e.g.*, Person, Rider, Car, Truck, Bus, Train, Motorcycle, Bicycle. Our new dataset can provide the prerequisite for the OVID task. Here, because of the labels, we utilize abbreviations instead of labels in order to easily show our results, *e.g.*, 'N, P' denotes the 'No-Intrusion, Person', Text prompt: Person. 'Y, C' denotes the 'Intrusion, Car', Text prompt: Car. 'Y, Bu' denotes the 'Intrusion, Bus', Text prompt: Bus. The detailed correspondence between full name, text prompt, and abbreviation is shown in Table 7.

(a) Original images (b) Segmentation-Label (c) Detection-Label (d) Ours(Intrusion & class & text label)

Figure 8: More visualization results of our Cityintrusion-OpenV. Unlike previous intrusion detection datasets (Sun et al., 2020; Han et al., 2024b), our datasets encompass all common/possible intrusion categories in Cityscape datasets, providing richer and varied labels that meet the requirements of the proposed OVID task.

A.3 More Intrusion Dataset Comparisons

In this subsection, we further compare our proposed datasets with other promising intrusion detection datasets and provide more comparison results to verify the superiority of our dataset, as shown

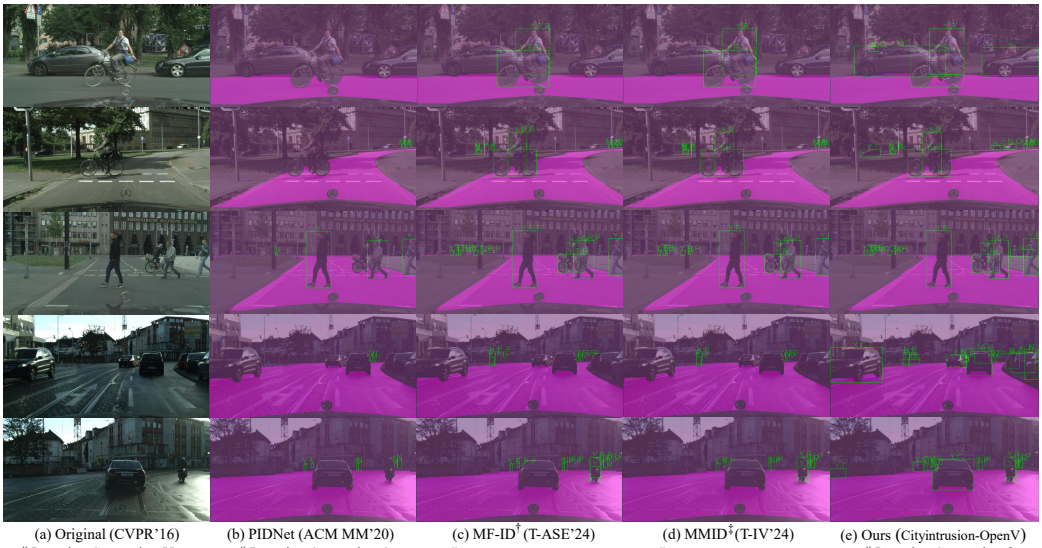

(a) Original (CVPR'16) # Intrusion Categories: **None** | (b) PIDNet (ACM MM'20) # Intrusion Categories: **1** | (c) MF-ID† (T-ASE'24) # Intrusion Categories: **4** | (d) MMID‡ (T-IV'24) # Intrusion Categories: **4** | (e) Ours (Cityintrusion-OpenV) # Intrusion Categories: **8**

Figure 9: The compression between our datasets with other promising intrusion detection datasets. Unlike previous intrusion datasets (Sun et al., 2020; Han et al., 2024b), our datasets encompass a broader range of potential intruders. Our datasets can be used to train/evaluate the performance of the OVID task and validate the effectiveness of the proposed strategies.

in Figure 9. Compared to previous promising intrusion detection datasets (Sun et al., 2020; Han et al., 2024b;c), our dataset exhibits much superior and richer labels. Besides, the proposed datasets contain **8** intrusion categories, surpassing the previous works **1** or **4** categories.More importantly, our Cityintrusion-OpenV dataset contains text labels, which compensate for the lack of relevant datasets and meet the needs of the proposed OVID task.

A.4 The Correspondence Between Full Name, Text Prompt, and Abbreviation

To better help understand the different intrusion categories and the abbreviations in our paper, we provide the detailed correspondence between the full name, the text prompt, and the abbreviation. The detailed correspondence is shown in the Table 7, *e.g.*, 'Person' (# Full name) → 'Person' (# Text prompt) → 'P' (# Abbreviation), 'Rider' (# Full name) → 'Rider' (# Text prompt) → 'R' (# Abbreviation), 'Car' (# Full name) → 'Car' (# Text prompt) → 'C' (# Abbreviation), 'Truck' (# Full name) → 'Truck' (# Text prompt) → 'Tk' (# Abbreviation), 'Bus' (# Full name) → 'Bus' (# Text prompt) → 'Bu' (# Abbreviation).

Table 7: The correspondence between the full name, text prompt, and abbreviation. *Italic* denotes *thing classes* (AoI). All categories are customizable in different scenarios.

# No.	# Full name	# Text prompt	# Abbreviation
# 1	'Person'	'Person'	'P'
# 2	'Rider'	'Rider'	'R'
# 3	'Car'	'Car'	'C'
# 4	'Truck'	'Truck'	'Tk'
# 5	'Bus'	'Bus'	'Bu'
# 6	'Train'	'Train'	'Tn'
# 7	'Motorcycle'	'Motorcycle'	'M'
# 8	'Bicycle'	'Bicycle'	'Bc'
# 9	'*Road*'	'*Road*'	'*Ro*'
# 10	⋮	⋮	⋮

A.5 Framework Design Motivation

In this subsection, We first explore two basic yet important questions as motivations for our approach. (1) **Why** do we conduct open vocabulary intrusion detection research? Our goal is to break through the dependencies and limitations of pre-defined categories. Truly enable intrusion detection in the open world. (2) **How** to achieve the specific OVID task? A simple idea is that we can leverage a collaborative model with Open-vocabulary segmentation (OVS), *e.g.*, SAM (Kirillov et al., 2023), FastSAM (Zhao et al., 2023), EfficientSAM (Xiong et al., 2024), and Open-vocabulary detection (OVD), *e.g.*, DetClip (Yao et al., 2023), Grounding DINO (Liu et al., 2023), YOLO-world (Cheng et al., 2024) to train/infer and get final Intrusion/No-intrusion labels. As shown in Table 8, we list and compare some feasible schemes. Unfortunately, although the model of 'OVD+OVS' is a feasible solution, it is not suitable for intrusion detection. The main reason is that the training cost of the End-to-End strategy combined with two **LLVMs** (Large Language Vision Models) is very expensive. To alleviate this problem, we design a new efficient framework for the proposed OVID task, namely OVIDNet. Our framework is established based on OpenSeeD (Zhang et al., 2023). Finally, the OVIDNet is leveraged to collaborate to give the bounding box and mask image for the OVID task, and the final intrusion labels ('N/Y') are given by the intrusion post-processing judgments. The overall framework and pipeline of OVIDNet are illustrated below.

Table 8: The comparison of some feasible schemes for the proposed OVID task. OVD and OVS denote the Open-vocabulary detection and segmentation models. Pre-trained TSM denotes the pre-trained traditional segmentation models, *e.g.*, DeepLabv3+ (Chen et al., 2018), PspNet (Zhao et al., 2017). Retrain denotes whether the model needs to be retrained under different scenarios. We can find that our scheme is End-to-End and has a low training cost.

Scheme	OVD		OVS		Pre-trained TSM	End-to-End	Open-Vocabulary?	Retrain	Training Cost
	Train	Infer	Train	Infer					
S1	✓	✓	✓	✓	✗	✗	✓	✗	Very Large
S2	✓	✓	✗	✗	✓	✓	✗	✓	Large
S3	✓	✓	✗	✓	✗	✗	✓	✗	Low
Ours	✓	✓	✓	✓	✗	✓	✓	✗	Low

B More Experiment Settings

In this section, we will introduce more implementation details and settings in the experiments. We present more setting details for the experiment, as shown in Table 9. Due to the limitation of our GPUs, we have to set the Image_size to 800 and reduce the iterations to 15000, which inevitably makes some of our results lower than those in the original model (image_size: 1200×1200, max_iter: 368750) (Zhang et al., 2023). To ensure fairness and verify the correctness of our method, we also set CHECKPOINT_PERIOD and EVAL_PERIOD to 15000, respectively, for all experiments. Additionally, we retrain the baseline and verify the method's validity. Note that our OVIDNet framework is built based on the OpenSeeD (Zhang et al., 2023). The OpenSeeD is a simple but efficient framework for open-vocabulary segmentation and detection. Differently, we modify the original framework to meet the requirements of the OVID task. We first add an effective intrusion detection judgment module to obtain the capability for intrusion detection. Then, we propose two strategies for improving generalization and intrusion performance in the open world and verify the effectiveness on multiple dominant datasets and tasks. Therefore, to be fair, our setting mainly refers to Openseed and is adapted to our own tasks. Our OVIDNet framework consists of a text encoder (Clip (Radford et al., 2021)), image encoder (Tiny-swin-transformer (Liu et al., 2021)), decoder, and intrusion detection post-processing module. Note that the final overlapping pixel threshold is set to 20 (Sun et al., 2020).

C More Results for OVID Task

In this section, we will provide additional results to evaluate and test the feasibility and effectiveness of our framework and strategies. We first report quantitative results of different categories in normal transfer conditions and cross-domain conditions. Then, we present more visualization results. The specific results are shown below.

Table 9: The detailed illustration of the experiment setting.

# Name 1	Setting Category 1	Value	# Name 2	Setting Category 2	Value
TOKENIZER	TEXT	CLIP	WINDOW_SIZE	BACKBONE	7
CONTEXT_LENGTH		18	PATCH_SIZE		4
WIDTH		512	EMBED_DIM		96
HEADS		8	DEPTHS		[2, 2, 6, 2]
LAYERS		12	NUM_HEADS		[3, 6, 12, 24]
# Name 3	Setting Category 3	Value	# Name 4	Setting Category 4	Value
IGNORE_VALUE	ENCODER	255	NHEADS	DECODER	8
LOSS_WEIGHT		1.0	CLASS_WEIGHT		4.0
CONVS_DIM		256	MASK_WEIGHT		5.0
MASK_DIM		256	DICE_WEIGHT		5.0
COMMON_STRIDE		4	BOX_WEIGHT		5.0
TRANSFORMER_ENC_LAYERS		6	GIOU_WEIGHT		2.0
TOTAL_NUM_FEATURE_LEVELS		4	HIDDEN_DIM		256
NUM_FEATURE_LEVELS		3	NUM_OBJECT_QUERIES		300

C.1 Quantitative Results of Different Categories

We first present additional results from various categories using the proposed strategies. Note that we give two types of metrics, *i.e.*, segmentation/detection metrics (IOU, AP, AP@.5) and intrusion detection metrics (AccY, AccN, Acc), respectively. The former is obtained via a zero-shot manner, the latter via a task-specific transfer manner. We conduct experiments in COCO, Cityscape, and Cityintrusion-OpenV, as shown in Table 10. From Table 10, we can find that when the proposed methodology is added, multiple metrics in multiple categories are improved to a certain extent. Compared with the baseline model, our strategies can surpass it by 3.4% (IOU), 1.0% (AP), and 1.4% (AP@.5), respectively, which verifies the effectiveness of the proposed strategies.

Table 10: The more quantitative results of different intrusion categories. Task: **COCO→Cityscape, Cityintrusion-OpenV**. We provide quantitative results for all possible intrusion categories to test the effectiveness of the proposed strategies. Additionally, to comprehensively measure the results across different categories, we report two distinct metrics, *i.e.*, segmentation/detection metrics (IOU, AP, AP@.5) and intrusion detection metrics (AccY, AccN, Acc), respectively. The **bold** is the best result.

-			**Intrusion Categories, Task: COCO→Cityscape, Cityintrusion-OpenV**								
Strategies			**Segmentation and Detection Metrics**								
Baseline	DMG	MDNM	Person(%)	Rider(%)	Car(%)	Truck(%)	Bus(%)	Train(%)	Motorcycle(%)	Bicycle(%)	**Avg**(%)
			IOU|AP|AP@.5	IOU|AP|AP@.5	IOU|AP|AP@.5	IOU|AP|AP@.5	IOU|AP|AP@.5	IOU|AP|AP@.5	IOU|AP|AP@.5	IOU|AP|AP@.5	IOU|AP|AP@.5
✓	✗	✗	64.7|9.1|23.8	0.0|0.0|0.0	80.8|17.2|36.7	24.0|18.6|25.3	62.8|36.1|53.9	2.2|13.7|25.4	45.8|10.3|25.1	69.6|10.4|30.4	43.74|14.43|27.58
✓	✗	✓	67.2|10.6|26.1	0.0|0.0|0.0	82.5|17.1|38.7	36.0|19.1|29.4	47.8|32.4|52.8	4.1|17.7|31.8	50.9|8.2|21.3	68.5|8.8|28.4	44.63|14.24|28.56
✓	✓	✗	69.9|12.3|32.1	0.0|0.0|0.0	80.1|21.4|45.5	24.2|14.5|20.5	51.0|36.2|53.1	0.6|12.5|20.0	56.1|10.7|25.7	72.2| 11.5|36.4	44.26|14.89|**29.16**
✓	✓	✓	66.5|11.0|28.6	0.0|0.0|0.0	86.5|22.8|47.0	37.4|22.1|32.9	60.2|33.3|45.4	0.0|9.6|13.6	58.6|11.9|27.8	72.5|12.2|36.5	**47.71**|**15.36**|28.97
Strategies			**Intrusion Detection Metrics**								
Baseline	DMG	MDNM	Person(%)	Rider(%)	Car(%)	Truck(%)	Bus(%)	Train(%)	Motorcycle(%)	Bicycle(%)	All Categories
			AccY |AccN|Acc	AccY|AccN|Acc	AccY|AccN|Acc	AccY|AccN|Acc	AccY|AccN|Acc	AccY|AccN|Acc	AccY|AccN|Acc	AccY|AccN|Acc	AccY|AccN|Acc
✓	✗	✗	12.43|46.39|39.28	0.00|0.00|0.00	22.74|29.48|25.88	30.77|7.32|20.43	31.34|35.48|32.65	0.00|0.00|0.00	14.55|21.28|18.79	12.19|38.70|30.55	18.72|36.19|29.36
✓	✓	✗	18.02|42.47|37.35	0.00|0.00|0.00	22.50|36.38|28.97	28.85|4.88|18.28	25.37|38.71|29.59	0.00|0.00|0.00	20.00|26.60|24.16	18.01|43.12|35.40	20.06|37.56|**30.72**
✓	✗	✓	21.51|39.99|36.12	0.00|0.00|0.00	22.70|42.87|32.10	21.15|14.63|18.28	35.82|32.26|34.69	11.11|7.14|8.70	12.73|23.40|19.46	20.22|42.26|35.49	21.01|38.64|**31.75**
✓	✓	✓	19.55|41.10|36.59	0.00|0.00|0.00	28.12|40.16|33.73	32.69|7.32|21.51	32.84|29.03|31.63	0.00|0.00|0.00	25.45|15.96|19.46	21.61|43.61|36.85	24.43|38.16|**32.79**

C.2 More Results of Cross-domain Task

Furthermore, we present additional intrusion detection results for various intrusion categories across different cross-domain tasks. In this experiment, we adopt three different foggy coefficients, *i.e.*, α=0.005, α=0.01, and α=0.02. In these experiments, We conduct experiments in COCO, Foggy-Cityscape, and Cityintrusion-OpenV, as shown in Table 11. We can observe that, in various cross-domain tasks, our strategies enhance intrusion detection performance. In four different tasks, compared with the original baseline model, our framework can improve them by 2.96%, 3.22%, and 3.45%, respectively. Furthermore, our proposed approach can effectively improve the performance of intrusion detection for various categories. These performance improvements demonstrate the effectiveness of our approach, as well as the ability of our framework to generalize.

Table 11: The more quantitative results of different intrusion categories in the cross-domain task. We further test the effectiveness of the proposed strategies with a task-specific transfer manner. Task: **COCO→Foggy-Cityscape, Cityintrusion-OpenV**. Three foggy conditions are used to conduct comprehensive experiments, *i.e.*, α=0.005,α=0.01,α=0.02. The **bold** is the best result.

-			Intrusion Categories, Task: COCO→Foggy-Cityscape, Cityintrusion-OpenV								
Strategies			α = **0.005**								
Baseline	DMG	MDNM	Person(%)	Rider(%)	Car(%)	Truck(%)	Bus(%)	Train(%)	Motorcycle(%)	Bicycle(%)	All Categories
			AccY|AccN|Acc	AccY|AccN|Acc	AccY|AccN|Acc	AccY|AccN|Acc	AccY|AccN|Acc	AccY|AccN|Acc	AccY|AccN|Acc	AccY|AccN|Acc	AccY|AccN|Acc
✓	✗	✗	14.11|45.14|38.64	0.00|0.00|0.00	25.43|24.38|24.94	28.85|4.88|18.28	31.34|29.03|30.61	0.00|0.00|0.00	9.09|20.21|16.11	10.25|37.10|28.85	20.43|33.58|28.44
✓	✓	✗	19.13|41.21|36.59	0.00|0.00|0.00	23.67|30.96|27.06	38.46|4.88|23.66	29.85|32.26|30.61	0.00|0.00|0.00	23.64|22.34|22.82	18.56|41.15|34.21	21.29|34.75|**29.49**
✓	✗	✓	20.39|38.18|34.45	0.00|0.00|0.00	24.07|38.68|30.88	26.92|12.20|20.43	31.34|29.03|30.61	0.00|7.14|4.35	14.55|27.66|22.82	20.22|40.66|34.38	21.66|36.20|**30.52**
✓	✓	✓	20.81|39.55|35.62	0.00|0.00|0.00	28.28|35.05|31.43	32.69|7.32|21.51	38.81|25.81|34.69	0.00|0.00|0.00	27.27|19.15|22.15	22.44|42.26|36.17	24.96|35.54|**31.40**
Strategies			α = **0.01**								
Baseline	DMG	MDNM	Person(%)	Rider(%)	Car(%)	Truck(%)	Bus(%)	Train(%)	Motorcycle(%)	Bicycle(%)	All Categories
			AccY|AccN|Acc	AccY|AccN|Acc	AccY|AccN|Acc	AccY|AccN|Acc	AccY|AccN|Acc	AccY|AccN|Acc	AccY|AccN|Acc	AccY|AccN|Acc	AccY|AccN|Acc
✓	✗	✗	14.53|41.66|35.98	0.00|0.00|0.00	26.11|20.84|23.66	30.77|4.88|19.35	29.85|19.35|26.53	0.00|0.00|0.00	14.55|20.21|18.12	13.30|36.12|29.11	21.29|30.64|26.98
✓	✓	✗	19.55|38.81|34.78	0.00|0.00|0.00	24.79|27.51|26.06	36.54|4.88|22.58	29.85|22.58|27.55	0.00|0.00|0.00	20.00|22.34|21.48	20.22|38.94|33.19	22.14|32.16|**28.24**
✓	✗	✓	21.09|36.81|33.52	0.00|0.00|0.00	25.31|33.53|29.14	28.85|7.32|19.35	35.82|29.03|33.67	11.11|7.14|8.70	18.18|27.66|24.16	22.99|39.07|34.13	23.00|33.56|**29.43**
✓	✓	✓	20.95|37.81|34.28	0.00|0.00|0.00	30.00|30.50|30.23	28.85|7.32|19.35	29.85|25.81|28.57	0.00|0.00|0.00	25.45|20.21|22.15	23.55|40.17|35.06	25.94|32.93|**30.20**
Strategies			α = **0.02**								
Baseline	DMG	MDNM	Person(%)	Rider(%)	Car(%)	Truck(%)	Bus(%)	Train(%)	Motorcycle(%)	Bicycle(%)	All Categories
			AccY|AccN|Acc	AccY|AccN|Acc	AccY|AccN|Acc	AccY|AccN|Acc	AccY|AccN|Acc	AccY|AccN|Acc	AccY|AccN|Acc	AccY|AccN|Acc	AccY|AccN|Acc
✓	✗	✗	14.53|37.22|32.47	0.00|0.00|0.00	26.96|14.86|21.32	30.77|2.44|18.28	28.36|12.90|23.47	0.00|0.00|0.00	20.00|20.21|20.13	15.24|30.96|26.13	22.04|25.88|24.38
✓	✓	✗	21.23|34.48|31.71	0.00|0.00|0.00	26.75|20.10|23.66	32.69|4.88|20.43	29.85|16.13|25.51	0.00|0.00|0.00	23.64|24.47|24.16	22.44|33.05|29.79	23.88|26.90|**25.72**
✓	✗	✓	23.60|33.07|31.09	0.00|0.00|0.00	27.96|26.36|27.21	30.77|2.44|18.28	35.82|19.35|30.61	11.11|7.14|8.70	16.36|20.21|18.79	27.42|33.54|31.66	25.51|28.50|**27.33**
✓	✓	✓	21.79|33.59|31.12	0.00|0.00|0.00	32.25|23.83|28.33	28.85|4.88|18.28	32.84|16.13|27.55	0.00|0.00|0.00	25.45|17.02|20.13	25.48|34.52|31.74	27.72|27.90|**27.83**

C.3 More Visualization Comparison Results

Finally, we also present more visualization comparison results to verify the effectiveness of the proposed framework and strategies. We set the text prompt of stuff_classes as Road and set the text prompt of thing_classes as'Person', 'Rider', 'Car', 'Truck', 'Bus', 'Train', 'Motorcycle', 'Bicycle', as shown in Figure 10. From Figure 10, we can find that our framework can present promising visualization detection results, not only detecting all intruders correctly but also giving correct Intrusion ('Y')/No-intrusion ('N') labels, which proves the effectiveness of our approach.

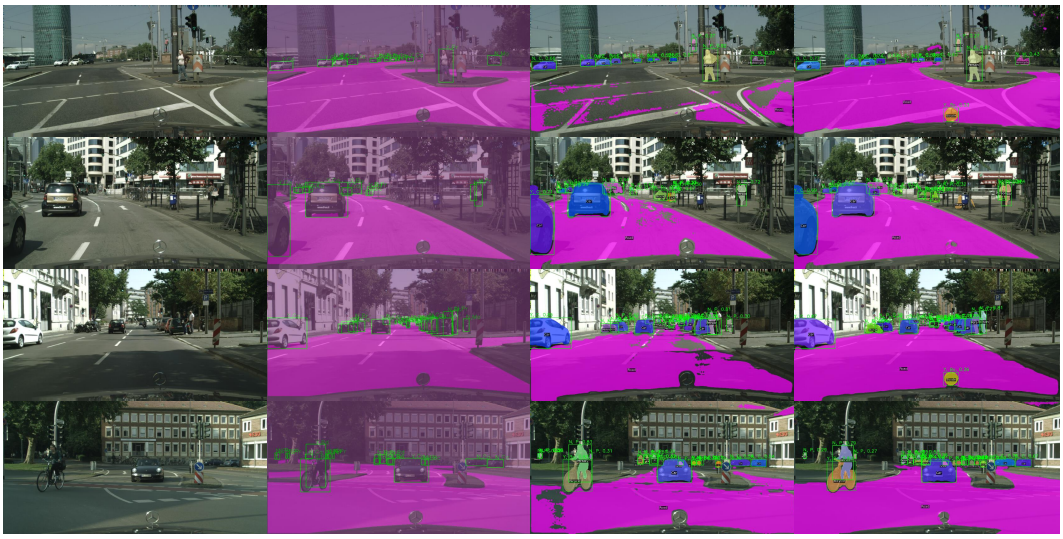

(a) Original images (b) Ground Truth (c) Baseline (d) Ours

Figure 10: The visualization comprising results. Here, (a), (b), (c), and (d) denote Original images, Ground truth, Baseline results, and Ours, respectively. Text prompt: Road (stuff_classes), 'Person', 'Rider', 'Car', 'Truck', 'Bus', 'Train', 'Motorcycle', 'Bicycle', (thing_classes). For thing_classes, the abbreviations are used instead of complete labels to easily show our results. The correspondence between the abbreviation and full name can be referred to in the Table 7.

D LIMITATION

In this paper, we introduce the Open-Vocabulary Intrusion Detection (OVID) project for the first time, including a new task, an efficient framework, and a strong benchmark for vision-based intrusion detection. Additionally, we design corresponding strategies to enhance intrusion detection performance in real-world scenarios and increase the practicality of the model. However, there are still some limitations that need to be addressed in the future, *e.g.*, enhance the ability to recognize fine-grained categories and improve generalization performance in the real world.

E MORE VISUALIZATION EXPERIMENTS RESULTS

Figure 11: More Visualization experiments results.

F LLM USAGE DISCLOSURE

In the preparation of this paper, we used the large language model to assist with language refinement, including improving and checking potential grammatical issues as well as enhancing clarity and readability. The model was not used to generate scientific content, ideas, experiments, or analyses. The authors take full responsibility for the accuracy and integrity of the paper's content.